Mon. Not. R. Astron. Soc. **000**, 1–5 (2011) Printed 27 January 2011 (MN LaTeX style file v2.2)

X-ray and optical observations of the closest isolated radio pulsar⋆

A. Tiengo,[1]† R.P. Mignani,[2] A. De Luca,[1,3] P. Esposito,[4,5] A. Pellizzoni[4] and S. Mereghetti[1]

[1]*INAF - Istituto di Astrofisica Spaziale e Fisica Cosmica - Milano, via E. Bassini 15, I-20133 Milano, Italy*
[2]*University College London, Mullard Space Science Laboratory, Holmbury St. Mary, Dorking, Surrey RH5 6NT, UK*
[3]*IUSS - Istituto Universitario di Studi Superiori, viale Lungo Ticino Sforza 56, I-27100 Pavia, Italy*
[4]*INAF - Osservatorio Astronomico di Cagliari, località Poggio dei Pini, strada 54, I-09012 Capoterra, Italy*
[5]*INFN - Istituto Nazionale di Fisica Nucleare, Sezione di Pavia, via A. Bassi 6, I-27100 Pavia, Italy*

Accepted 2010 December 26. Received 2010 December 20; in original form 2010 October 7

ABSTRACT

With a parallactic distance of 170 pc, PSR J2144–3933 is the closest isolated radio pulsar currently known. It is also the slowest (P = 8.51 s) and least energetic ($\dot{E}_{\rm rot} = 2.6 \times 10^{28}$ erg s^{-1}) radio pulsar; its radio emission is difficult to account for with standard pulsar models, since the position of PSR J2144–3933 in the period–period derivative diagram is far beyond the typical radio 'death lines'. Here we present the first deep X-ray and optical observations of PSR J2144–3933, performed in 2009 with *XMM-Newton* and European Southern Observatory (ESO)/Very Large Telescope (VLT), from which we derive, assuming a blackbody emission spectrum, a surface temperature upper limit of 2.3×10^5 K for a 13 km radius neutron star, 4.4×10^5 K for a 500 m radius hot spot and 1.9×10^6 K for a 10 m radius polar cap. In addition, our non-detection of PSR J2144–3933 constrains its non-thermal luminosity to be $<$30 per cent and $<$2 per cent of the pulsar rotational energy loss in the 0.5–2 keV X-ray band and in the B optical band, respectively.

Key words: stars: neutron – pulsars: individual: PSR J2144–3933.

1 INTRODUCTION

The radio pulsar PSR J2144–3933, discovered in the Parkes Southern Pulsar Survey (Young, Manchester & Johnston 1999), stands out among the nearly 2000 radio pulsars catalogued so far for several reasons. Its spin period (P) of 8.51 s is the longest of any known radio pulsars. The rotation parameters of PSR J2144–3933 are such that its radio emission is surprising: its period and period derivative ($\dot{P} \simeq 4 \times 10^{-16}$ s s^{-1}, corrected for the 'Shklovskii effect'; Shklovskii 1970) values locate PSR J2144–3933 in the P–$\dot{P}$ diagram below most proposed 'death lines' (e.g. Chen & Ruderman 1993), where the accelerating potential is below the minimum value required to produce pair cascades and thus radio emission. Its radio emission has been explained either by proposing new models for pair production in the magnetosphere (Zhang et al. 2000) or by suggesting that strong multipolar surface magnetic fields are present in all radio pulsars (Gil & Mitra 2001).

PSR J2144–3933 has one of the largest characteristic ages ($\tau_c = P/(2\dot{P}) \simeq 3.4 \times 10^8$ years) among non-recycled radio pulsars and the lowest rotational energy loss ($\dot{E}_{\rm rot} = 4\pi^2 I \dot{P} P^{-3} \simeq 2.6 \times 10^{28}$ erg s^{-1}, where $I \approx 10^{45}$ g cm^2 is the moment of inertia of the neutron star) of any pulsar. The magnetic field, computed assuming magnetodipolar spin-down, is $B = \sqrt{\frac{3c^3 I}{8\pi R^6} P\dot{P}} \simeq 1.9 \times 10^{12}$ G, which instead is close to the average value for non-recycled radio pulsars.

A very faint object at radio wavelengths (apparent luminosity of $\sim$20 μJy kpc^2 at 1400 MHz; Deller et al. 2009), PSR J2144–3933 could be detected thanks to its small distance, only $\sim$180 pc as inferred from a dispersion measure of 3.35 cm^{-3} pc assuming the Galactic free electron density model of Taylor & Cordes (1993). This led Young, Manchester & Johnston (1999) to propose that PSR J2144–3933 could be the tip of the iceberg of a huge population of Galactic long-period and low-luminosity pulsars, very difficult to detect but comparable in number to previous estimates of the total pulsar population of the Galaxy. A much more robust distance of 165^{+17}_{-14} pc,[1] based on the pulsar parallax, as well as precise position ($<$1 mas) and proper motion measurement, $\mu_\alpha = -57.89 \pm 0.88$ mas yr^{-1} and $\mu_\delta = -155.9 \pm 0.54$ mas yr^{-1}, were recently obtained trough very long baseline interferometry (VLBI) observations at the Australian Long Baseline Array

⋆ Based on observations obtained with *XMM-Newton*, an ESA science mission with instruments and contributions directly funded by ESA Member States and NASA, and with ESO/*VLT* Antu (UT1).

† E-mail: tiengo@iasf-milano.inaf.it

[1] Correcting for the Lutz–Kelker bias (Lutz & Kelker 1973), the distance of PSR J2144–3933 is only slightly increased to 172^{+20}_{-15} pc (Verbiest, Lorimer & McLaughlin 2010).

(Deller et al. 2009). At the time of writing, according to the continuously updated on-line ATNF Pulsar Catalogue (Manchester et al. 2005),[2] PSR J2144–3933 is the closest isolated radio pulsar.

Despite its small distance, PSR J2144–3933 has never been detected outside of the radio waveband. Here we present the first deep optical and X-ray observations of PSR J2144–3933, performed in 2009 with ESO/*VLT* and *XMM-Newton*.

2 X-RAY DATA ANALYSIS AND RESULTS

XMM-Newton observed PSR J2144–3933 for about 40 ks on 2009 October 24. Since the aim of the observation was the search for X-ray emission from the pulsar, only the data collected by the EPIC instrument, composed by three imaging detectors sensitive in the 0.2–15 keV energy range, were analysed.[3] The EPIC PN camera (Strüder et al. 2001) was operated in full frame mode, while the two EPIC MOS units (Turner et al. 2001) were operated in large window mode. The thin optical blocking filter was used for the three EPIC cameras. All the data were processed using the *XMM-Newton* Science Analysis Software (SAS version 9.0.0). To improve the sensitivity at the lowest energy, where thermal emission from PSR J2144–3933 is more likely to be detectable, the PN data were further processed using the SAS tool EPREJECT,[4] which substantially reduces the low energy instrumental background due to electronic noise. The standard pattern selection criteria for the EPIC X–ray events (patterns 0–4 for PN and 0–12 for MOS) were adopted. After filtering out the time intervals affected by a high level of particle background, the net exposure times were 22 ks for the PN and 26 ks for the MOS.

A blind search for X-ray emission from PSR J2144–3933 was performed using different source detection algorithms in many energy bands, but no source compatible with the pulsar position was detected. The closest X-ray source is 25.6 ± 0.5 arcsec away from the proper-motion-corrected position of PSR J2144–3933 (Deller et al. 2009, see Figure 1), while the absolute astrometry of the EPIC images is $\sim$1 arcsec (root mean square, rms).[5]

In order to set an upper limit on the pulsar X-ray emission, we selected the events from a 10 arcsec radius circular region centred at the position of PSR J2144–3933, obtaining, in the 0.2–10 keV energy range, 40 and 21 counts in the PN and in the two MOS cameras summed together, respectively (see Table 1 for other energy bands). To better characterise the background intensity in different energy bands, we extracted for each camera the background events from a larger source-free region in the same chip, deriving the estimates reported in Table 1 for the number of background events expected in the source region. Taking into account these background estimates and the Poissonian fluctuations (Gehrels 1986) of the counts extracted from the region of PSR J2144–3933, we obtain the 3σ upper limits on the pulsar count rate in different energy bands reported in Table 1. The conversion from count rates to fluxes for each detector is performed by assuming different spectral models (see Section 4) within the XSPEC (version 11.3.1) spectral fitting software and using the response matrices and ancillary files produced by the SAS software for a 10 arcsec circular region centred at the pulsar position.

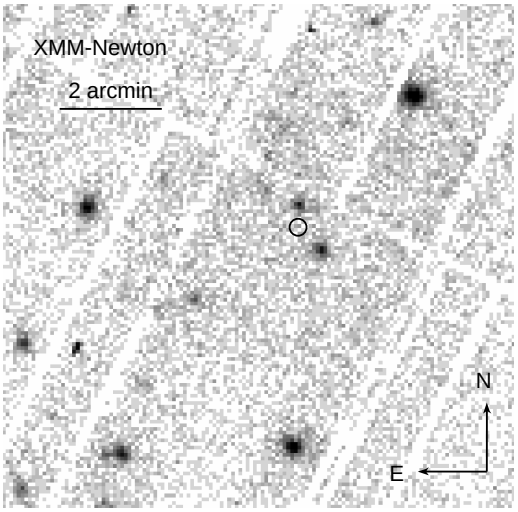

Figure 1. *XMM-Newton* EPIC image of the $\sim$10$\times$10 arcmin^2 field around PSR J2144–3933 in the 0.2–1 keV energy range. The predicted position of the pulsar (Deller et al. 2009) is marked by a 10 arcsec radius circle.

Table 1. The 3σ upper limits on the PSR J2144–3933 count rates in different energy bands in the PN and the sum of the two MOS cameras (last column). These limits are derived from the number of events detected within 10 arcsec from PSR J2144–3933 (third column) and the number of background counts expected in the same region (fourth column).

Energy band (keV)	Instrument	Observed counts	Background counts	$3\,\sigma$ upper limit (cts/s)
0.2–0.5	PN	5±2.2	6.8±0.5	4.9×10^{-4}
	MOS	5±2.2	2.4±0.1	5.4×10^{-4}
0.5–2	PN	15±3.9	10.1±0.6	1.0×10^{-3}
	MOS	8±2.8	7.4±0.2	5.4×10^{-4}
2–10	PN	20±4.5	16.7±0.8	1.1×10^{-3}
	MOS	8±2.8	8.4±0.2	5.0×10^{-4}
0.2–10	PN	40±6.3	33.6±1.1	1.5×10^{-3}
	MOS	21±4.6	18.3±0.4	8.3×10^{-4}

3 OPTICAL DATA ANALYSIS AND RESULTS

We observed PSR J2144–3933 with the *VLT* at the ESO Paranal observatory on 2009 August 21 in visitor mode with *FOcal Reducer/low dispersion Spectrograph* (*FORS2*) at the Cassegrain focus of the Antu UT1 telescope. To enhance the sensitivity in the blue part of the spectrum, we used the *FORS2* blue-sensitive CCD detector, a mosaic of two $2k \times 4k$ E2V CCDs (with 15 μm pixels) optimised for wavelengths shorter than 6000 Å. In its standard resolution mode, the detector has a pixel size of 0.25 arcsec (2$\times$2 binning) which corresponds to a projected field of view of $8\farcm3\times8\farcm3$ over the CCD mosaic. To include a larger number of reference stars for a precise image astrometry and photometry calibration, as well as to increase the signal-to-noise ratio per pixel, we performed the observations in standard resolution mode. We positioned the pulsar in the upper CCD chip to exploit its larger effective sky coverage (7×4 arcmin^2). We chose the standard low gain, fast read-out

[2] See http://www.atnf.csiro.au/research/pulsar/psrcat/

[3] PSR J2144–3933 was also simultaneously observed with the Optical Monitor (Mason et al. 2001) for 36 ks with the UVW1 filter, but the observation was not sensitive enough to constrain significantly the pulsar emission.

[4] See http://xmm.esac.esa.int/sas/current/doc/epreject/index.html.

[5] See http://xmm2.esac.esa.int/docs/documents/CAL-TN-0018.pdf.

CCD mode. We observed the target through the high-throughput U ($\lambda = 3610$ Å; $\Delta\lambda = 505.1$ Å), B ($\lambda = 4400$ Å; $\Delta\lambda = 1035.1$ Å), and V ($\lambda = 5570$ Å; $\Delta\lambda = 1235$ Å) filters. A few bright stars located relatively close to the pulsar position were masked to avoid ghost images and saturation spikes. We performed three sequences of five 590 s exposures each for a total integration time of 8850 s through both the U and B filters and a sequence of five 590 s exposures through the V filter (2950 s integration time) in dark time, photometric sky conditions, and average air masses of $\sim$1.05, $\sim$1.14, and $\sim$1.29 in the U, B, and V filters, respectively. The measured image quality (IQ) is ~ 0.8 arcsec in both the U and B filters and $\sim$0.98 arcsec in the V one.

We acquired bias and twilight flat–field frames according to the *FORS2* science calibration plan and images of standard star fields (Landolt 1992) We reduced the science and standard star images using the last version of the ESO *FORS2* data reduction pipeline[6] after producing master bias and flat–field frames. For each filter, reduced science images were stacked and averaged using available tools in *MIDAS*. We computed the photometric zero point using the *FORS2* pipeline. Unfortunately, since the E2V detector is mounted at *FORS2* only during visitor mode runs, no standard star observations are routinely taken to monitor the stability of the zero point and to compute the extinction coefficients in different filters. However, we could use as a reference the average extinction coefficients computed for the E2V detector mounted at *FORS1*.[7] We estimate that the error on the zero point is $\sim$0.1 magnitude at most, likely smaller than the expected photometric error expected for a target as faint as the pulsar. As a reference for the PSR J2144–3933 position we used the proper-motion-corrected VLBI coordinates obtained by Deller et al. (2009). To accurately overlay the pulsar coordinates, we have then re-computed the astrometric solution of the *FORS2* image, using as a reference objects selected from the Guide Star Catalogue 2 (GSC-2; Lasker et al. 2008). After accounting for the rms of the astrometric fit ($\sigma_{\rm r} = 0.13$ arcsec), the uncertainty of the registration of the *FORS2* image on the GSC-2 reference frame ($\sigma_{\rm tr} = 0.13$ arcsec), and the 0.15 arcsec uncertainty on the link of the GSC-2 to the International Celestial Reference Frame (ICRF), we estimate that the overall (1σ) uncertainty of our astrometry is $\delta_r = 0.24$ arcsec.

The position of PSR J2144–3933 is shown in Fig. 2, overlaid on the co-added *FORS2* B-band image. As seen, the pulsar position falls close to a rather bright source which is also detected in the U and V-band images. Its coordinates, $\alpha = 21^{\rm h}44^{\rm m}11\overset{\rm s}{.}97$, $\delta = -39^\circ33'56\overset{''}{.}42$, imply an offset of $\sim$ 1.2 arcsec from the computed pulsar position at the epoch of our *VLT* observations, i.e. 7 times larger than the overall uncertainty of our astrometric solution. Thus, we can safely rule out that this object is associated to the pulsar. Its magnitudes, measured through customised aperture photometry with SEXTRACTOR, are $U = 23.39 \pm 0.05$, $B = 23.82 \pm 0.03$, $V = 23.76 \pm 0.05$, after correcting for the air mass. Its colours suggest that the object (Object A) might be a background star, or, more likely, a galaxy, as suggested by its somewhat patchy morphology. We could not detect any other object close to the pulsar radio position in any of the *FORS2* U, B, and V-band images. The estimate of the upper limit is complicated by wings of Object A's PSF which extend at the pulsar radio position. The possible extended nature of such object does not allow us to perform simple PSF subtraction. Thus, we used a different approach. We simulated a point source (modelled as a Gaussian, with a FWHM equal to the value measured for non-extended objects on our final coadded images), subtracted it at the expected pulsar position, and estimated the resulting residuals on the image in an aperture with a diameter equal to the FWHM. Such an exercise was repeated using increasing values for the magnitude of the simulated source, until residuals were consistent with a 3σ negative fluctuation. After correcting for atmospheric extinction, the resulting upper limits to the emission of PSR J2144−3933 are $U > 25.3$, $B > 26.6$, and $V > 25.5$.

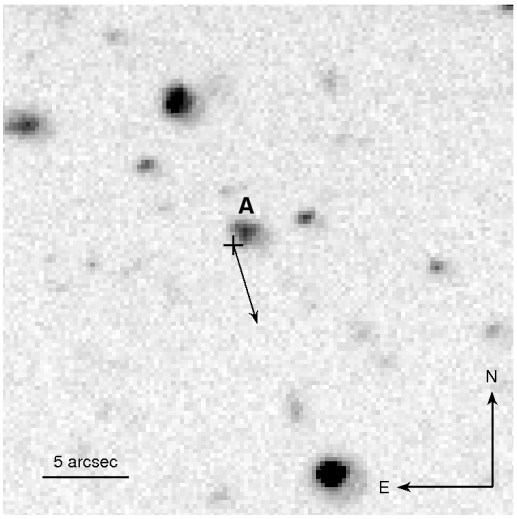

Figure 2. ESO/*VLT* B-filter image of the $\sim$30$\times$30 arcsec^2 field around PSR J2144–3933, whose predicted position is marked by a cross. The arrow indicates the proper motion direction and its length corresponds to the movement of PSR J2144–3933 in 30 years (Deller et al. 2009). Object A, which is likely a background galaxy, is also indicated.

4 DISCUSSION AND CONCLUSIONS

PSR J2144–3933 being the closest isolated radio pulsar currently known, its non-detection in our deep *XMM-Newton* and *VLT* observations sets robust upper limits on its X-ray and optical luminosity. Thanks to the high sensitivity of the *XMM-Newton* PN instrument in the soft X-ray band, the best constraints on the thermal emission from PSR J2144–3933 can be obtained from the PN data in the 0.2–0.5 keV band (see Table 1 and Fig. 3). Given the 170 pc distance, assuming a column density of $N_{\rm H} = 10^{20}$ cm^{-2} (as inferred from the radio dispersion measure for a 10 per cent ionization of the interstellar medium) and blackbody emission from the whole surface of a 13 km radius neutron star, the 3σ upper limits on the temperature[8] is 2.3×10^5 K ($kT = 20$ eV). However, the neutron star temperature is not expected to be uniform, with the magnetic poles hotter than the rest of the surface. The radius of the polar cap can be estimated as $R_{\rm pc} = (2\pi R^3/cP)^{1/2} \sim 50$ m, where $R = 10$ km is the neutron star radius and $P = 8.51$ s is the pulse period. Significantly smaller emitting regions are expected, e.g., in the partially screened gap model (Gil et al. 2008) and possibly observed in the thermal emission of old pulsars (e.g., Pavlov et al.

[6] See http://www.eso.org/observing/dfo/quality/FORS2/pipeline.
[7] See http://www.eso.org/observing/dfo/quality/FORS1/qc/qc1.html.
[8] The blackbody temperatures and radii reported here are the values measured at infinity. An observed radius of 13 km corresponds to an intrinsic radius of $\sim$10 km for a 1.4 $M_\odot$ neutron star.

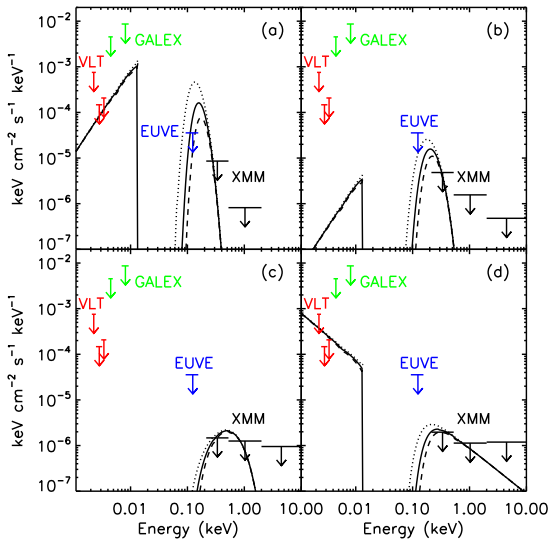

Figure 3. 3σ upper limits on the flux of PSR J2144–3933 derived from our *VLT* and *XMM-Newton* observations and from archival *EUVE* and *GALEX* data. The models used to derive the X-ray upper limits are shown for different values of interstellar extinction (REDDEN model in XSPEC) and absorption (PHABS in XSPEC) by the dotted [$E(B-V) = 0.01$; $N_{\rm H} = 5\times10^{19}$ cm^{-2}], solid [$E(B-V) = 0.02$; $N_{\rm H} = 10^{20}$ cm^{-2}] and dashed [$E(B-V) = 0.03$; $N_{\rm H} = 1.5\times10^{20}$ cm^{-2}] lines: blackbody with temperature $T = 2.3\times10^5$ K and emission radius of 13 km (a), with temperature $T = 4.4\times10^5$ K and 500 m radius (b), with temperature $T = 1.9\times10^6$ K and 10 m radius (c), and power-law with photon index $\Gamma = 2$ and 0.5–2 keV luminosity of 7×10^{27} erg s^{-1} (d).

2009). Assuming a 10 m radius polar cap, we obtain a temperature upper limit of 1.9×10^6 K ($kT = 165$ eV) and a bolometric luminosity $L < 10^{28}$ erg/s. Our non-detection therefore implies a polar cap efficiency $L/\dot{E}_{\rm rot} < 0.4$, not particularly constraining considering that efficiencies <1 per cent are typically observed in rotation-powered pulsars. On the other hand, much larger hot spots are inferred from the X-ray spectra of isolated neutron stars possibly heated by magnetic field decay (Kaplan & van Kerkwijk 2009), which might be related to PSR J2144–3933 (see below). Assuming a 500 m radius hot spot, we obtain a blackbody temperature upper limit of 4.4×10^5 K ($kT = 38$ eV) and a bolometric luminosity $L < 7\times10^{28}$ erg/s.

PSR J2144–3933 was not detected in the extreme UV in a deep 20 ks observation with *EUVE* (Korpela & Bowyer 1998). The flux upper limit of 0.023 μJy at 100 Å is below the extrapolation to the extreme UV of the $T = 2.3\times10^5$ K blackbody spectrum from the whole neutron star surface, if $N_{\rm H} = 10^{20}$ cm^{-2} is assumed. However, Fig. 3 shows how the constraints derived from the *EUVE* data strongly depend on the interstellar absorption, while the presumably low absorption and extinction towards this nearby pulsar has no impact in the X-ray and optical band. We also compared the extrapolation in the optical of the same blackbody spectrum with our *VLT* flux upper limits. Our deepest limit, obtained through the B filter, is a factor of ≈ 2 above the Rayleigh-Jeans tail of the X-ray blackbody spectrum, absorbed by an interstellar reddening $E(B-V) = 0.02$.[9] Thus, it does not constrain the neutron star surface temperature. The PSR J2144–3933 field was observed in direct image mode by *GALEX* (Martin et al. 2005) during the all-sky survey for an exposure time of 208 s but no source was detected at the pulsar position down to a 3σ flux limit of ~ 3 μJy and ~ 6 μJy in the *GALEX* NUV ($\lambda = 2771$ Å; $\Delta\lambda = 500$ Å) and FUV band ($\lambda = 1528$ Å; $\Delta\lambda = 200$ Å), respectively. As can be seen in Fig. 3, these limits are well above the hottest blackbody compatible with the *XMM-Newton* data.

Our limit of 2.3×10^5 K is among the lowest currently available for the surface temperature of a neutron star. Considering typical cooling models (see Yakovlev & Pethick 2004 for a review) and the characteristic age of PSR J2144–3933 (3.4×10^8 years) the neutron star surface temperature is expected to be $<10^5$ K. Possible evidence of surface temperature higher than expected from cooling models has been found for the 200 Myr old PSR J0108−1431 (Mignani et al. 2008; Pavlov et al. 2009; Deller et al. 2009). Moreover, the peculiar position of PSR J2144–3933 in the pulsar period–period derivative diagram suggests a possible non-standard evolution and thus a more complex cooling history. For example, this long period pulsar might be the descendant of a magnetar, i.e. a neutron star powered by the decay of its internal magnetic field of 10^{14-15} G (see Mereghetti 2008 for a review). In this hypothesis, the initially stronger magnetic field would have slowed down the neutron star cooling (Arras et al. 2004) and, at the same time, the field decay would have heated up the neutron star surface either through Joule heating (e.g., Miralles et al. 1998) or possible magnetar-like bursting episodes. Moreover, in case of field decay, PSR J2144–3933 would be much younger than its characteristic age, which largely overestimates the pulsar age when the magnetic field decreases with time. This possibility is apparently precluded by the low dipolar magnetic field of PSR J2144–3933 ($B = 1.9\times10^{12}$ G), since numerical simulations of magnetic field decay in neutron stars have shown that the field decay should virtually stop at a field intensity of $\sim$2–3$\times10^{13}$ G (Pons et al. 2009). However, the recent discovery of a transient X-ray source with timing parameters similar to those of PSR J2144–3933 (P=9.1 s, $\dot{P}<6\times10^{-15}$ s s^{-1}, and thus a dipolar magnetic field $B<7.5\times10^{12}$ G) showing magnetar-like activity indicates that a strong internal magnetic field might power the high energy emission of isolated neutron stars with dipolar magnetic fields well below 10^{13} G (Rea et al. 2010). The X-ray dim isolated neutron stars (XDINSs, see Haberl 2007 for a review), which are nearby neutron stars with similarly long pulsation periods and surface temperatures of 5–12$\times10^5$ K, have also been suggested to be aged magnetars (see, e.g., Popov et al. 2010). When a period derivative has been measured, characteristic ages of 1–4$\times10^6$ years and dipolar magnetic fields of 1–3$\times10^{13}$ G have been derived. Although our non-detection of PSR J2144–3933 cannot exclude the possibility that this radio pulsar was born as a magnetar, it indicates that, in this scenario, it would be older than the XDINSs, as already suggested by its lower dipolar magnetic field and longer characteristic age.

PSR J2144–3933 being the radio pulsar with the lowest rotational energy loss, the search for non-thermal emission from this object is challenging as well. Assuming a power-law spectrum with photon index $\Gamma = 2$ (see the lowermost panel of Figure 3), we can derive a 3σ upper limit on the 0.5–2 keV observed flux of 1.9×10^{-15} erg cm^{-2} s^{-1} from the PN data and 2.5×10^{-15} erg cm^{-2} s^{-1} from the combined data of the two MOS units. The upper limit on the pulsar non-thermal luminosity in the 0.5–2 keV energy range is 7×10^{27} erg s^{-1}, corresponding to $\sim$30 per cent of its rotational energy loss. This limit is not particularly constraining, since the efficiency to convert pulsar spin-down power into X-ray lumi-

[9] This value for the reddening is computed using the relation of Predehl & Schmitt (1995) and assuming $N_{\rm H} = 10^{20}$ cm^{-2}.

nosity is observed to be typically much lower (Li et al. 2008). The *VLT* B-band upper limit corresponds to a luminosity $\lesssim 5.6 \times 10^{26}$ erg s^{-1}, which is $\lesssim$2 per cent of the spin-down luminosity. This is about 4 orders of magnitude above the rotation-powered optical emission efficiency of pulsars with comparable spin-down age. For instance the old pulsars PSR B1929+10 ($\sim 3\times10^6$ years) and PSR B0950+08 ($\sim 17 \times 10^6$ years) have optical emission efficiencies of $\approx 10^{-6}$ and $\approx 4 \times 10^{-6}$ (Zharikov et al. 2006), respectively.

To improve the *XMM-Newton* temperature upper limit by a factor of ~ 2, optical observations deeper by at least ~ 1.5 magnitudes would be required. Although these observations are within reach of the *VLT*, they are complicated by the presence of Object A, ~ 1.2 arcsec away from the pulsar position. This would require an image quality much better than 0.8 arcsec, which is challenging for ground-based optical observations. A substantial improvement in sensitivity to surface thermal emission from PSR J2144–3933 can instead be obtained with near-UV observations with the *HST*, which, apart from having a much better angular resolution, would take advantage from a more favorable waveband, around the peak of a $T<10^5$ K blackbody spectrum.

Considering that PSR J2144–3933 is a nearby neutron star and that Object A is a relatively bright (B=23.8) background source (probably a galaxy), their small angular separation might cause a detectable gravitational lensing effect (see, e.g., Paczynski 1996b). The displacement (or deformation, being the object slightly extended) of the background source due to the gravitational field of a point-like mass is expected to be (Paczynski 1996a)

$$\delta\varphi = \frac{\varphi_E^2}{\Delta\varphi}, \quad (1)$$

where φ_E is the Einstein ring radius and $\Delta\varphi$ is its angular distance from the lens. In the approximation of a very distant lensed object, the Einstein radius for a lens with mass M at a distance D is

$$\varphi_E = \left(\frac{4GM}{c^2 D}\right)^{1/2}. \quad (2)$$

Although the proximity of PSR J2144–3933 ($D = 170$ pc) and its relatively small angular separation from Object A ($\Delta\varphi = 1.2$ arcsec) make it the most favorable case for any known neutron star, for a mass of 1.4 $M_\odot$ a displacement of only $\delta\varphi = 0.06$ mas is expected. Given the large and well constrained proper motion of PSR J2144–3933, two precise measurements of the galaxy apparent position in different epochs would be enough to measure its displacement and therefore to obtain a measure of the neutron star mass. Unfortunately, the astrometric precision of currently available optical instruments is not adequate for such a measurement. In the future, a sufficient angular resolution might be reachable, but this measure will not be possible anymore because the direction of the pulsar proper motion, which is opposite to the background object position and is not going to intercept any other bright source in the next decades (see Fig. 2), will make the required precision rapidly increasing with time. Together with the other nearby neutron stars with a well determined proper motion, PSR J2144–3933 is anyway a good candidate for the measure of a neutron star mass through microlensing (see, e.g., Dai et al. 2010). In fact, deeper observations, for example with the *HST* or the forthcoming *JWST*, might find dimmer sources along its sky trajectory, which, observed at their closest approach to the pulsar, might either show a displacement or a flux increase. This measurements would be less challenging in the case of PSR J2144–3933 than for the other nearby neutron stars, thanks to its vanishing flux outside the radio band.

ACKNOWLEDGEMENTS

We thank the referee, J. Gil, for his helpful comments and G. Mathys for his support in executing the *VLT* observations. We acknowledge the partial support from ASI (ASI/INAF contract I/088/06/0). PE acknowledges financial support from the Autonomous Region of Sardinia through a research grant under the program PO Sardegna FSE 2007–2013, L.R. 7/2007.

REFERENCES

Arras P., Cumming A., Thompson C., 2004, ApJ, 608, L49
Chen K., Ruderman M., 1993, ApJ, 402, 264
Dai S., Xu R. X., Esamdin A., 2010, MNRAS, 405, 2754
Deller A. T., Tingay S. J., Bailes M., Reynolds J. E., 2009, ApJ, 701, 1243
Gehrels N., 1986, ApJ, 303, 336
Gil J., Haberl F., Melikidze G., Geppert U., Zhang B., Melikidze Jr. G., 2008, ApJ, 686, 497
Gil J., Mitra D., 2001, ApJ, 550, 38
Haberl F., 2007, Ap&SS, 308, 181
Kaplan D. L., van Kerkwijk M. H., 2009, ApJ, 705, 798
Korpela E. J., Bowyer S., 1998, AJ, 115, 2551
Landolt A. U., 1992, AJ, 104, 340
Lasker B. M., et al., 2008, AJ, 136, 735
Li X., Lu F., Li Z., 2008, ApJ, 682, 1166
Lutz T. E., Kelker D. H., 1973, PASP, 85, 573
Manchester R. N., Hobbs G. B., Teoh A., Hobbs M., 2005, AJ, 129, 1993
Martin D. C., et al., 2005, ApJ, 619, L1
Mason K. O., et al., 2001, A&A, 365, L36
Mereghetti S., 2008, A&A Rev., 15, 225
Mignani R. P., Pavlov G. G., Kargaltsev O., 2008, A&A, 488, 1027
Miralles J. A., Urpin V., Konenkov D., 1998, ApJ, 503, 368
Paczynski B., 1996a, ARA&A, 34, 419
Paczynski B., 1996b, Acta Astronomica, 46, 291
Pavlov G. G., Kargaltsev O., Wong J. A., Garmire G. P., 2009, ApJ, 691, 458
Pons J. A., Miralles J. A., Geppert U., 2009, A&A, 496, 207
Popov S. B., Pons J. A., Miralles J. A., Boldin P. A., Posselt B., 2010, MNRAS, 401, 2675
Predehl P., Schmitt J. H. M. M., 1995, A&A, 293, 889
Rea N., Esposito P., Turolla R., Israel G. L., Zane S., Stella L., Mereghetti S., Tiengo A., Götz D., Göğüş E., Kouveliotou C., 2010, Science, 330, 944
Shklovskii I. S., 1970, Soviet Astronomy, 13, 562
Strüder L., et al., 2001, A&A, 365, L18
Taylor J. H., Cordes J. M., 1993, ApJ, 411, 674
Turner M. J. L., et al., 2001, A&A, 365, L27
Verbiest J. P. W., Lorimer D. R., McLaughlin M. A., 2010, MNRAS, 405, 564
Yakovlev D. G., Pethick C. J., 2004, ARA&A, 42, 169
Young M. D., Manchester R. N., Johnston S., 1999, Nature, 400, 848
Zhang B., Harding A. K., Muslimov A. G., 2000, ApJ, 531, L135
Zharikov S., Shibanov Y., Komarova V., 2006, Advances in Space Research, 37, 1979

This paper has been typeset from a TEX/ LATEX file prepared by the author.